

Effect of proton irradiation on the normal state low-energy excitations of $\text{Ba}(\text{Fe}_{1-x}\text{Rh}_x)_2\text{As}_2$ superconductors

M. Moroni,^{1,*} L. Gozzelino,^{2,3} G. Ghigo,^{2,3} M. A. Tanatar,⁴ R. Prozorov,⁴ P. C. Canfield,⁴ and P. Carretta¹

¹*Department of Physics, University of Pavia-CNISM, I-27100 Pavia, Italy*

²*Istituto Nazionale di Fisica Nucleare, Sez. Torino, Torino 10125, Italy*

³*Politecnico di Torino, Dept. of Applied Science and Technology, 10129 Torino, Italy*

⁴*Ames Laboratory USDOE and Department of Physics and Astronomy, Iowa State University, Ames, Iowa 50011, USA*

We present a ^{75}As Nuclear Magnetic Resonance (NMR) and resistivity study of the effect of 5.5 MeV proton irradiation on the optimal electron doped ($x = 0.068$) and overdoped ($x = 0.107$) $\text{Ba}(\text{Fe}_{1-x}\text{Rh}_x)_2\text{As}_2$ iron based superconductors. While the proton induced defects only mildly suppress the critical temperature and increase residual resistivity in both compositions, sizable broadening of the NMR spectra was observed in all the irradiated samples at low temperature. The effect is significantly stronger in the optimally doped sample where the Curie Weiss temperature dependence of the line width suggests the onset of ferromagnetic correlations coexisting with superconductivity at the nanoscale. $1/T_2$ measurements revealed that the energy barrier characterizing the low energy spin fluctuations of these compounds is enhanced upon proton irradiation, suggesting that the defects are likely slowing down the fluctuations between $(0, \pi)$ and $(\pi, 0)$ nematic ground states.

PACS numbers: 74.70.Xa, 76.60.-k

I. INTRODUCTION

Chemical substitution is the most common approach used to introduce impurities in strongly correlated electron systems in order to probe their local response function. However, this method often gives rise to structural distortions, unwanted inhomogeneity and to charge doping. Accordingly, in order to study the effect of the bare impurities the right dopant must be carefully chosen and the options are often very limited. Thus irradiation with energetic particles, electrons and ions, may represent a powerful alternative to chemical substitutions. Radiation induced defects have been extensively employed in high temperature superconductors to investigate the pair breaking effect of non magnetic scattering centers and to study the pinning of the Abrikosov vortices. In particular, heavy ions irradiation (e.g. with Au and Pb) induces strongly anisotropic columnar defects, which are effective in pinning the flux vortices^{1,2}. Conversely, low mass ions, such as protons, α particles or electrons, give rise to uniformly distributed point like defects whose density can be precisely controlled. In the cuprates the decrease of the superconducting transition temperature T_c with the radiation fluence ϕ was found to strongly depend on the ion type, on its energy and on the total dose³. Remarkably, in $\text{YBa}_2\text{Cu}_3\text{O}_{7-\delta}$ and $\text{Tl}_2\text{Ba}_2\text{CuO}_{6+x}$, it was found⁴ that the defects introduced by electron irradiation play a role analogous to nonmagnetic Zn impurities and the magnitude of $dT_c/d\phi$ is consistent with the theoretical prediction for a d -wave superconductor⁵.

In the iron based superconductors (IBS) several irradiation studies have been conducted with heavy^{2,6-12} ions, light ions^{9,11,13,14} and electrons¹⁵⁻²⁰. In these compounds T_c suppression by radiation damage is rather weak for optimally doped compositions but becomes stronger in under-doped and overdoped compositions. Simultane-

ous studies of T_c suppression and London penetration depth as a function of doping in $\text{Ba}_{1-x}\text{K}_x\text{Fe}_2\text{As}_2$ ^{16,19} conclude that both quantities can be reasonably fit to s^\pm model^{21,22} which is the leading candidate for describing the pairing state in most of the IBS²³⁻²⁵. Interestingly, these results are consistent with the reduced T_c suppression induced by non-magnetic Zn doping in $\text{Ba}(\text{Fe}_{1-x}\text{Co}_x)_2\text{As}_2$ and $\text{LaFeAsO}_{1-x}\text{F}_x$ ²⁶⁻²⁹. This weak effect of diamagnetic impurities in IBS is not necessarily an indication of a different gap symmetry. In fact one should notice that the defects weaken also the spin density wave (SDW) phase competing with superconductivity (SC) in the underdoped part of the phase diagram^{23,30,31}. Hence, $dT_c/d\phi$ strongly depends on the system parameters in the underdoped regime, both for proton irradiation and nonmagnetic Zn doping^{13,14,26-29}.

The studies cited above focus mainly on the superconducting state and no reports can be found in the literature on a systematic investigation of the effects of irradiation on the normal state properties of IBS, in particular on the spin and nematic correlations³². In 122 iron based superconductors very slow spin fluctuations have been detected above T_c with Nuclear Magnetic Resonance (NMR)³³⁻³⁵ and have been ascribed to nematic fluctuations among $(0, \pi)$ and $(\pi, 0)$ correlated regions³⁶. Recently ^{75}As $1/T_2$ NMR measurements in the electron doped $\text{Ba}(\text{Fe}_{1-x}\text{Rh}_x)_2\text{As}_2$ revealed^{37,38} that these fluctuations are not only present in the underdoped part of the phase diagram but extend up to at least 11% Rh doping, well into the overdoped regime.

In this manuscript we show that proton induced defects significantly affect the slow spin fluctuations revealed by ^{75}As $1/T_2$ in $\text{Ba}(\text{Fe}_{1-x}\text{Rh}_x)_2\text{As}_2$, suggesting that the fluctuations developing between $(0, \pi)$ and $(\pi, 0)$ phases are affected by the disorder. Moreover, we observe a broadening of the ^{75}As NMR spectra induced by proton irradiation and for the optimally doped 0.068 Rh

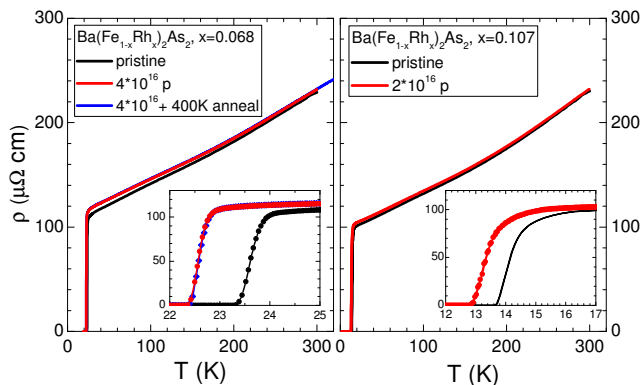


FIG. 1. (Color online) Temperature-dependent electrical resistivity $\rho(T)$ of optimally doped $x=0.068$ (left panel) and overdoped $x=0.107$ (right panel) samples of $\text{Ba}(\text{Fe}_{1-x}\text{Rh}_x)_2\text{As}_2$. Insets zoom into superconducting transition range. Black lines show $\rho(T)$ for samples in the pristine state, red lines show the data for the same samples after proton irradiation. Blue line in left panel shows $\rho(T)$ of the same sample after annealing at 400 K, revealing permanent character of proton irradiation damage, in contrast to damage by electron irradiation¹⁶. Note non-parallel shift of the $\rho(T)$ curves after irradiation, revealing Matthiessen rule violation.

sample it evidenced that the defects induce ferromagnetically correlated regions around the impurities, coexisting with superconductivity.

II. EXPERIMENTAL METHODS AND RESULTS

The measurements presented in this work were performed on $\text{Ba}(\text{Fe}_{1-x}\text{Rh}_x)_2\text{As}_2$ single crystals with Rh content of $x = 0.068$ (optimally doped sample) and $x = 0.107$ (overdoped sample). The crystals were grown using the method described in Ref. 39. The samples were then characterized by means of resistivity and SQUID magnetometry measurements. Electrical resistivity measurements were made using four-probe technique on cleaved samples with typical dimensions $2 \times 0.5 \times 0.05 \text{ mm}^3$, with long dimension corresponding to [100] crystallographic direction. Low resistance contacts to the samples were made by soldering $50 \mu\text{m}$ Ag wires using Sn⁴⁰⁻⁴². Measurements were made on 6 samples of $x=0.068$ and 7 samples of $x=0.107$. In both cases resistivity of the samples at room temperature $\rho(300\text{K})$ was $230 \pm 30 \mu\Omega\text{cm}$, consistent within error bars with the results for Co-doped compositions of similar x ⁴³. Selected crystals of each batch were then irradiated with 5.5 MeV protons at the CN Van de Graaff accelerator of INFN-LNL (Istituto Nazionale di Fisica Nucleare - Laboratori Nazionali di Legnaro, Italy). Contacts to the samples remained intact during irradiation, thus eliminating uncertainty of geometric factor determination and enabling quantitative comparison of resistivity measurements. To minimize the heating of the crystals under irradiation the proton flux was always

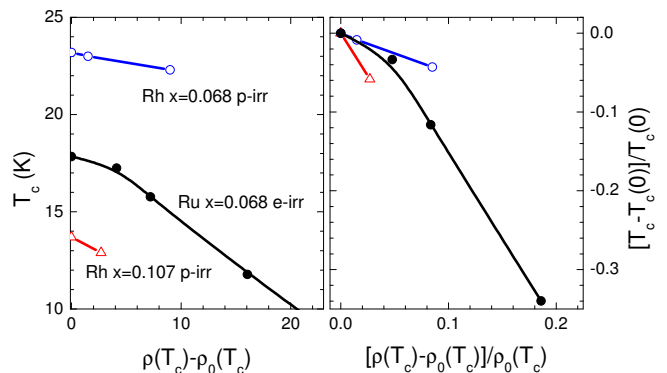


FIG. 2. (Color online) (Left panel) The superconducting transition temperature T_c as a function of change in sample resistivity $\rho(T_c)$ for samples of $\text{Ba}(\text{Fe}_{1-x}\text{Rh}_x)_2\text{As}_2$ with optimal doping $x=0.068$ (blue curve, open circles) and $x=0.107$ (red curve, open up-triangles). For reference we show data for iso-electron substituted $\text{Ba}(\text{Fe}_{1-x}\text{Ru}_x)_2\text{As}_2$ at optimal doping $x=0.24$, subjected to low-temperature 2.5 MeV electron irradiation, Ref. 16. Right panel shows same data plotted as a change in T_c and resistivity $\rho(T_c)$ normalized by their values in pristine samples $T_c(0)$ and $\rho_0(T_c)$.

limited to $10^{12} \text{ cm}^{-2} \text{ s}^{-1}$. The irradiation with 5.5 MeV protons produces random point defects and some defect nanoclusters, due to elastic scattering of protons against the target nuclei. The thickness of the crystals was much smaller than the proton implantation depth, as calculated by the SRIM-2013 code⁴⁴ using the Kinchin-Pease approach. This ensured a homogeneous defect distribution in the superconductor, as evidenced by Fig. 3c where the energy lost by protons due to elastic scattering is plotted as a function of the implantation depth. In Table I the average displacement damage and the inferred average distance between proton-induced point defects are reported as a function of the irradiation fluence. It has to be noted that this distance should be assumed as a lower limit since the primary point defects (Frenkel pairs) could migrate to form small clusters and some defects could anneal out. After crossing the whole crystals thickness protons get implanted into the sample-holder.

After irradiation the samples were again characterized with resistivity measurements to check the reduction of T_c and ⁷⁵As NMR measurements were then carried out. Figure 1 shows temperature dependent resistivity of the

TABLE I. Summary of the average displacements per atom (dpa) and distance between defects as a function of the proton irradiation fluences.

ϕ (cm^{-2})	dpa	Inter-defect distance (nm)
2×10^{16}	5.1×10^{-4}	3.5
3.2×10^{16}	8.2×10^{-4}	3
4×10^{16}	1×10^{-3}	2.8
6.4×10^{16}	1.6×10^{-3}	2.4

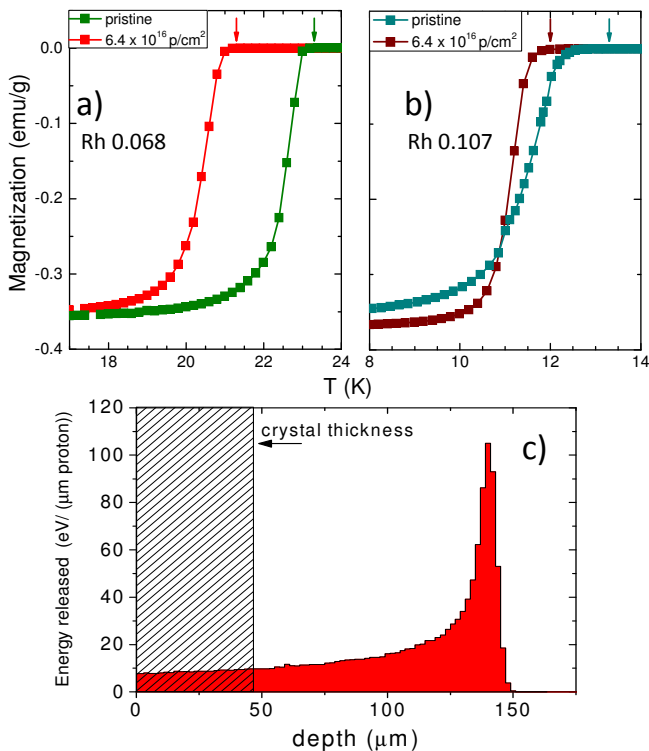


FIG. 3. (Color online) a) and b): SQUID magnetization measurements for the $x=0.068$ sample (a) and $x=0.107$ sample (b) carried out before and after irradiation. The arrows indicate T_c as determined by the onset of diamagnetism. c): Distribution of the proton energy loss in the superconducting crystals (less than $50 \mu\text{m}$ thick) as a function of depth. The thickness of the thickest irradiated sample is about $45 \mu\text{m}$, as evidenced in the picture. Therefore, the energy release can be considered homogeneous throughout the crystals, as well as the distribution of defects.

samples $x=0.068$ (left panel) and $x=0.107$ (right panel) before and after irradiation. Sample $x=0.068$ was subject to a fluence up to $4 \times 10^{16} \text{ cm}^{-2}$, which resulted in approximately 1 K decrease of T_c from 23.3 K to 22.3 K as determined by zero resistance criterion. Resistivity above the transition increased from 106 to 115 $\mu\Omega\text{cm}$. To check the stability of irradiation damage, sample of $x=0.068$ was heated up to 400 K. This protocol is known to show significant T_c restoration and residual resistivity decrease in electron irradiated samples¹⁶, none of which is observed for proton irradiation. Due to a two times smaller irradiation fluence, $2 \times 10^{16} \text{ cm}^{-2}$, T_c suppression in sample of $x=0.107$ is somewhat smaller, $\Delta T_c \approx 0.8 \text{ K}$, from 13.7 to 12.9 K. Resistivity increase is also notably smaller, $\Delta \rho \approx 3 \mu\Omega\text{cm}$. It should be noticed that, for both compositions, the resistivity increase after irradiation is not a rigid offset as one would expect from Matthiessen rule. The shift becomes notably larger at low temperatures, in line with observations on hole-doped $\text{Ba}_{1-x}\text{K}_x\text{Fe}_2\text{As}_2$ ¹⁸. In Fig. 2 we plot the effect of irradiation on T_c as a function of the residual resistivity change with respect to pristine sample $\rho(T_c) - \rho_0(T_c)$. In the right panel we plot the

same data normalized by the values in pristine sample. For reference we plot the data for iso-electron substituted $\text{Ba}(\text{Fe}_{1-x}\text{Ru}_x)_2\text{As}_2$ at optimal doping $x=0.24$, irradiated with 2.5 MeV electrons¹⁶. The rates of T_c variation are comparable in both cases, with some differences which can be ascribed to the variation of response due to the variation of doping level, rather than to the type of disorder. This is quite remarkable considering the very different annealing effect in the two cases.

T_c was also measured *in situ* during the NMR experiment by monitoring the detuning temperature of the NMR probe resonating circuit. The decrease of T_c after irradiation ($\phi = 3.2 \times 10^{16} \text{ cm}^{-2}$) was found to be small both for the $x=0.068$ (from 23.3 K before irradiation to $\sim 22 \text{ K}$ afterwards) and for the $x=0.107$ (from $\sim 13.3 \text{ K}$ to $\sim 12.5 \text{ K}$). The samples were then irradiated again to increase the total fluence to $\phi = 6.4 \times 10^{16} \text{ cm}^{-2}$, and SQUID (see Fig. 3a and 3b) and NMR measurements were repeated. The expected displacement damage after these second irradiations and the corresponding average distance between proton-induced point defects are reported in Table I. The second irradiation lowered T_c to 21.3 K for $x=0.068$ and to 12 K for $x=0.107$. Hence, the T_c decrease rate is $dT_c/d\phi \simeq 0.3 \times 10^{-16} \text{ K}\cdot\text{cm}^2$ for the optimally doped sample and about $0.2 \times 10^{-16} \text{ K}\cdot\text{cm}^2$ for the overdoped one.

The values of $dT_c/d\phi$ are lower than those observed in $\text{Ba}(\text{Fe}_{1-x}\text{Co}_x)_2\text{As}_2$ and $\text{Ba}_{1-x}\text{K}_x\text{Fe}_2\text{As}_2$ irradiated with 3 MeV protons^{13,14}. This effect was expected since the non-ionizing energy loss, which drives the number of defect produced per incoming proton, decreases with increasing proton energy³. This means that, somewhat counterintuitively, the effectiveness of protons in damaging the lattice decreases by increasing their energy.

For each sample doping and dose value we measured the temperature dependence of the ^{75}As NMR linewidth, of the spin-lattice relaxation rate ($1/T_1$) and of the spin-spin relaxation rate ($1/T_2$). The magnetic field $\mathbf{H}_0 = 7 \text{ T}$ was applied along the crystallographic c axis unless otherwise specified.

The full width at half maximum ($\Delta\nu$ hereafter) of the ^{75}As central line ($m_I = \frac{1}{2} \rightarrow -\frac{1}{2}$) was derived from the Fast Fourier Transform of half of the echo signal after a standard Hahn spin-echo ($\pi/2 - \tau - \pi$) pulse sequence. The results for the optimally doped sample are shown in Fig. 4 and those for the overdoped crystal can be found in Fig. 5. In the $x=0.068$ sample the linewidth increases significantly on cooling, following a Curie-Weiss law for all doses. Conversely, for $x=0.107$, $\Delta\nu$ remains nearly flat down to T_c in the non-irradiated sample while it slowly increases, reaching a maximum around 20 K, in the irradiated one. These strikingly different $\Delta\nu$ behaviors will be discussed in the next section.

The ^{75}As spin-lattice relaxation rate was estimated by fitting the recovery of the longitudinal magnetization $M_z(t)$ after a saturation recovery pulse sequence ($\pi/2 - \tau - \pi/2 - \tau_{\text{echo}} - \pi$) with the standard recovery

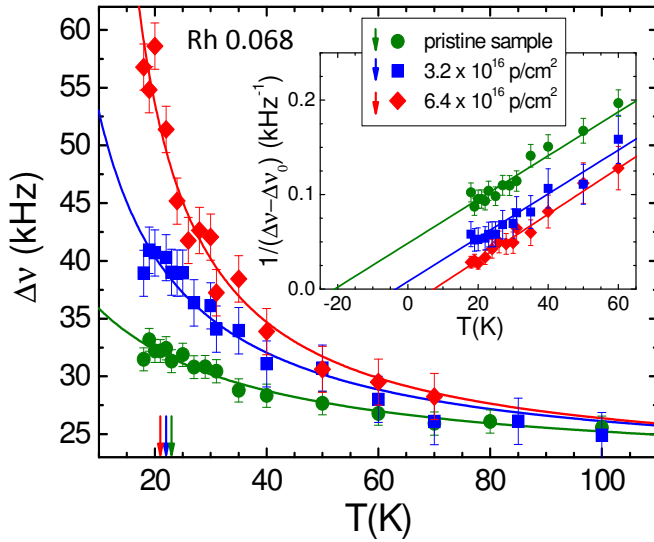


FIG. 4. (Color online) Temperature dependence of the Full Width at Half Maximum $\Delta\nu$ for the ^{75}As central line in the $x = 0.068$ sample. The solid lines are fits to a Curie-Weiss law (see text). Inset: Inverse of the temperature dependent component of the line width. The intercepts of the linear fits with the x axis correspond to $-\theta$ (see text). The arrows indicate T_c for each radiation dose.

function for the central line of a spin 3/2 nucleus:

$$M_z(\tau) = M_0[1 - f(0.1 \cdot e^{-(\tau/T_1)} + 0.9 \cdot e^{-(6\tau/T_1)})]. \quad (1)$$

The results, displayed in Fig. 6, clearly show that $1/T_1$ is unaffected by the presence of proton induced defects. In particular, the spin-lattice relaxation follows a power-law $1/T_1 \sim T^\alpha$, with $\alpha \simeq 0.6$ for the $x = 0.068$ sample and $\alpha \simeq 1$ for the $x = 0.107$ sample, namely close to the Korringa behavior expected for a weakly correlated metal.

The spin echo decay rate ($1/T_2$) was evaluated by recording the decay of the spin-echo amplitude $M_{total}(2\tau)$ after a spin echo pulse sequence. Since at high temperatures the values of T_1 and T_2 are in the same range (5-100 ms), the T_1 contribution to the spin echo decay is not negligible (Redfield term⁴⁵). Within this framework the echo decay amplitude $M_{total}(2\tau)$ can be written as⁴⁶:

$$M_{total}(2\tau) = M(2\tau) \exp\left(-\frac{2\tau}{T_{1R}}\right) \quad (2)$$

where $M(2\tau)$ is the T_1 independent echo decay amplitude while the exponential term takes into account the T_1 contribution. Walstedt and coworkers⁴⁶ found that, for the central line of a 3/2 spin nucleus, $1/T_{1R}$ is:

$$\frac{1}{T_{1R}} = \frac{3}{T_1^\parallel} + \frac{1}{T_1^\perp}, \quad (3)$$

where T_1^\parallel and T_1^\perp denote the spin lattice relaxation rate measured with the static magnetic field parallel and perpendicular to the crystallographic c axis, respectively.

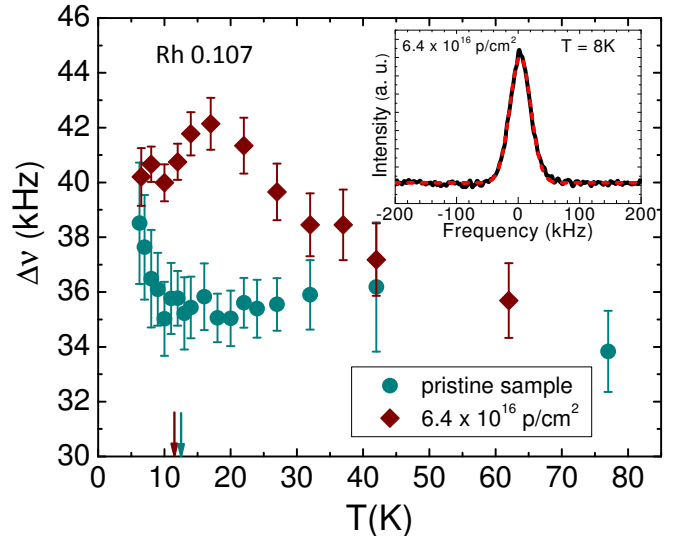


FIG. 5. (Color online) Temperature dependence of the linewidth (FWHM) for the ^{75}As central line in the $x = 0.107$ sample. In the inset a low temperature ^{75}As NMR spectrum is shown, the dashed line is a fit to a gaussian function. The arrows indicate T_c for each radiation dose. The line width data for the $\phi = 3.2 \times 10^{16} \text{ cm}^{-2}$ dose level are pretty similar to those for $\phi = 6.4 \times 10^{16} \text{ cm}^{-2}$ and have not been reported to improve the figure readability.

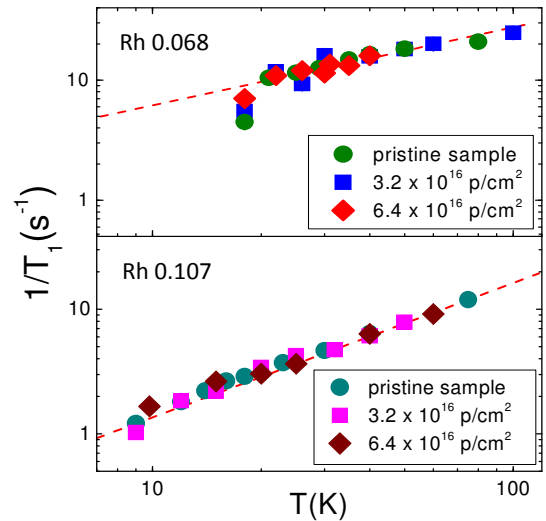


FIG. 6. (Color online) Temperature dependence of the ^{75}As $1/T_1$ measured with $\text{H} \parallel c$ for the $x = 0.068$ (top) and $x = 0.107$ (bottom) samples. The red dashed lines are guides to the eye.

The raw echo amplitude was then divided by $\exp(-\frac{2\tau}{T_{1R}})$ in order to derive $M(2\tau)$. It was found that $M(2\tau)$ deviates from a single exponential decay (see Fig. 7) and could be fitted, over the whole temperature range, by a

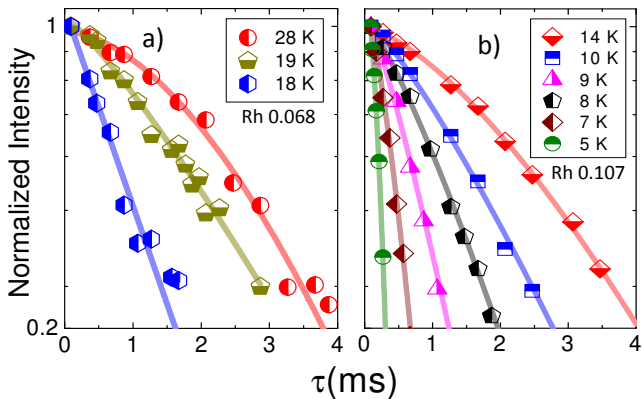


FIG. 7. Spin Echo decay amplitude $M(2\tau)$ for the optimally doped $x = 0.068$ (a) and over-doped $x = 0.107$ (b) samples irradiated with a fluence of $6.4 \times 10^{16} \text{ cm}^{-2}$, after dividing for Redfield contribution (see text). The solid lines are fits to a stretched exponential decay function (see text).

stretched exponential:

$$M(2\tau) = M_0 \exp\left(-\left(\frac{2\tau}{T_2}\right)^\beta\right), \quad (4)$$

with β the stretching exponent. The values of β are strongly temperature dependent (Fig. 7): at high temperature $\beta \simeq 2$, indicating a Gaussian decay of the spin echo, while it gradually decreases upon lowering the temperature, reaching $\beta \simeq 1$ (simple exponential) close to T_c . The temperature dependence of $1/T_2$ upon varying the dose and Rh doping is displayed in Fig. 8. While at temperatures much higher than T_c the spin echo decay rate is flat for both compounds, a sharp rise in $1/T_2$ was observed just above T_c . This effect has already been reported in previous studies (see Refs. 37 and 38) and is clearly decoupled from T_c . In fact, by increasing the static magnetic field³⁸ it is possible to shift the $1/T_2$ increase to much higher temperatures. As it can be seen in insets of Fig. 8, the $1/T_2$ upturn becomes sharper in the proton irradiated samples. If we define T^* as the temperature below which $T_2(100\text{K})/T_2 > 1$, one can observe that in both samples T^* decreases upon proton irradiation.

III. DISCUSSION

Let us first consider the rich phenomenology displayed by the ^{75}As NMR line width (Figs. 4 and 5). In the optimally doped sample ($x=0.068$) $\Delta\nu$ increases at low temperature for all the dose levels (see Fig. 4). Conversely, $\Delta\nu$ is flat at high temperature ($T > 60$ K) and its value is only weakly dependent on the total proton fluence. In the former compound it is possible to fit the line width temperature dependence with a Curie Weiss law:

$$\Delta\nu = \Delta\nu_0 + \frac{C}{T + \theta} \quad (5)$$

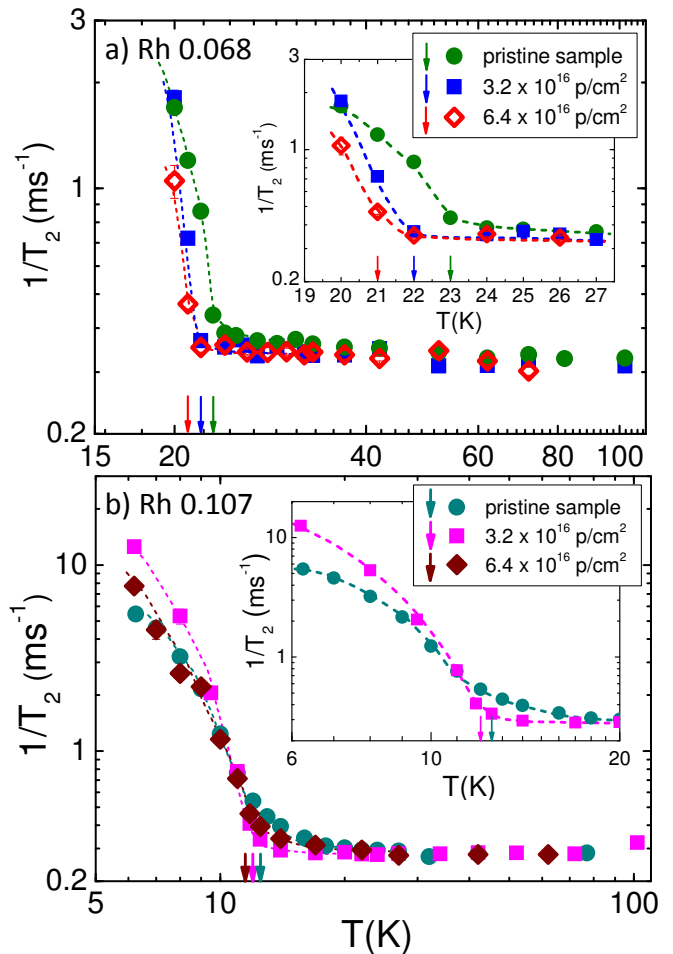


FIG. 8. (Color online) Temperature dependence of the ^{75}As $1/T_2$ relaxation rate of the $x = 0.068$ (top) and $x = 0.107$ (bottom) samples for different values of fluence (see legend). In the insets the low temperature data are shown in greater detail. The arrows indicate T_c for each radiation dose and Rh doping level. The dashed lines are guides to the eye.

where $\Delta\nu_0$ is a temperature independent component, C is the Curie constant and θ the Curie-Weiss temperature. The fit parameters are summarized in Table II. The Curie Weiss behavior of the linewidth and the observation that for $T < 50$ K $\Delta\nu$ decreases upon decreasing the magnetic field intensity indicate that the low temper-

TABLE II. Curie constant C and Curie-Weiss temperature θ obtained from the analysis of the temperature evolution of the ^{75}As NMR central line width $\Delta\nu$ shown in Fig. 4 for $\text{Ba}(\text{Fe}_{0.932}\text{Rh}_{0.068})_2\text{As}_2$. The temperature independent term $\Delta\nu_0$ is equal to 21.5 kHz.

ϕ (cm^{-2})	C (kHz·K)	θ (K)
0	420 ± 40	20 ± 4
3.2×10^{16}	460 ± 50	5 ± 3
6.4×10^{16}	440 ± 40	-6.5 ± 1.5

ature broadening is associated with the modulation of the local magnetic field at the nuclei induced by the electron spin texture.

The high temperature line width, $\Delta\nu_0 \simeq 21.5$ kHz, is due to the sum of nuclear dipolar line broadening, of the quadrupolar broadening and possibly of the magnetic broadening ($\Delta\nu_{\text{magnetic}} \propto M(T, H_0) \propto \chi(T)H_0$). From dipolar sums it can be found that the nuclear dipolar contribution is actually very small (< 2 kHz)^{37,47}. The quadrupolar broadening should be zero for $H \parallel c$, however the misalignment by an angle ϑ may lead to some broadening of the central ^{75}As NMR line, which can be estimated from⁴⁸

$$\Delta\nu_{0Q} \sim \frac{3\nu_Q \Delta\nu_Q \vartheta^2}{\nu_L}, \quad (6)$$

where ν_Q is the splitting between the central line ($\frac{1}{2} \rightarrow \frac{-1}{2}$) and the satellite line ($\frac{1}{2} \rightarrow \frac{3}{2}$), $\Delta\nu_Q$ the width of the satellite, $\nu_L = \gamma H_0 / 2\pi$ the Larmor frequency. The spectrum of the $\text{Ba}(\text{Fe}_{0.932}\text{Rh}_{0.068})_2\text{As}_2$ high frequency satellite line is reported in Fig. 9. If one considers that the misalignment $\vartheta < 10^\circ$ one finds that the quadrupolar broadening $\Delta\nu_{0Q} \leq 10$ kHz, still much smaller than $\Delta\nu_0$. It is then likely that the temperature independent magnetic broadening has to be associated with the T-independent component of the electron spin susceptibility, similarly to what reported by Mukhopadhyay et al.⁴⁷ in $\text{Ba}_{1-x}\text{K}_x\text{Fe}_2\text{As}_2$.

The Curie-Weiss $\Delta\nu$ behavior indicates the presence of spin correlations and was often observed in the cuprates in the presence of defects⁴⁹. In fact, the impurities induce a local spin polarization $\langle S_z \rangle$ on the conduction electrons which leads to a spatially varying spin polarization $s(\mathbf{r}) = \chi(\mathbf{r})\langle S_z \rangle$. The resulting NMR spectrum is the histogram of the spin polarization probed by the nuclei and the line width at a given temperature depends on the temperature evolution of $\chi(\mathbf{r})$. Accordingly, $\Delta\nu$ follows the susceptibility of the local moments which can be described by a Curie-Weiss law⁴⁹.

Remarkably, for $\phi = 6.4 \times 10^{16} \text{ cm}^{-2}$, the Curie-Weiss temperature becomes negative, signaling the shift of the correlations from antiferromagnetic to ferromagnetic. Ferromagnetic correlations were detected in other compounds of the 122 family, in particular in the non-superconducting $\text{Ba}(\text{Fe}_{1-x}\text{Mn}_x)_2\text{As}_2$ ⁵⁰ and, with a much lower θ , in the superconducting $\text{Ba}(\text{Fe}_{1-x}\text{Co}_x)_2\text{As}_2$ and $\text{BaFe}_2(\text{As}_{1-x}\text{P}_x)_2$ ⁵¹ after the introduction of Mn impurities. Ferromagnetic fluctuations were also observed in hole and electron doped BaFe_2As_2 ⁵² and in $\text{Ca}(\text{Fe}_{1-x}\text{Co}_x)_2\text{As}_2$ ⁵³. The observed $\Delta\nu$ temperature dependence is analogous to the one measured in Mn-doped $\text{LaFe}_{1-y}\text{Mn}_y\text{AsO}_{1-x}\text{F}_x$, where the introduction of tiny amounts of Mn strongly suppresses T_c and gives rise to a significant increase of ^{19}F NMR line width^{54,55}. However, in $\text{LaFe}_{1-y}\text{Mn}_y\text{AsO}_{1-x}\text{F}_x$, θ is always positive and the introduction of magnetic impurities enhances both θ and C , indicating that Mn doping strengthens the spin correlations already present in the Mn free compound. On the

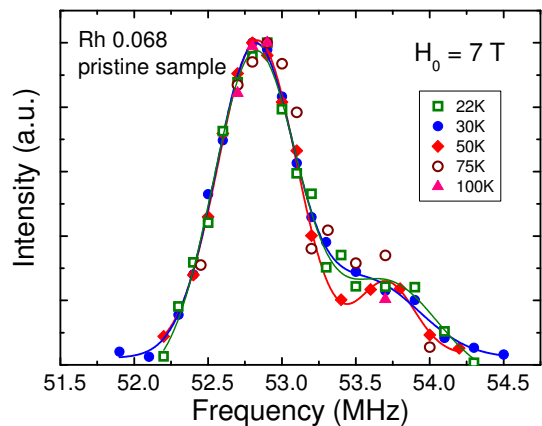


FIG. 9. (Color online) Spectra of the high frequency satellite line of $\text{Ba}(\text{Fe}_{0.932}\text{Rh}_{0.068})_2\text{As}_2$ for various temperatures. The intensity is the integral of the spin echo and the solid lines are fits to a double Gaussian.

other hand, in proton irradiated $\text{Ba}(\text{Fe}_{0.932}\text{Rh}_{0.068})_2\text{As}_2$, the value of C remains unchanged and θ first decreases and then changes sign upon increasing the dose.

It should be noticed that, at variance with Mn doping, the lattice defects created by proton irradiation are non-magnetic. Even though the rise of magnetism upon ion irradiation was observed in several materials⁵⁶ and we recall that the Ba122 family of iron-based superconductors is quite unstable towards impurity driven static magnetism^{47,57}. Hence, the observation that the nonmagnetic defects introduced by irradiation lead to enhanced spin correlations and to a broadening of the NMR lines is not unexpected. Indeed, it is well known that by doping $\text{YBaCu}_3\text{O}_{6+x}$ with nonmagnetic Zn impurities the ^{89}Y NMR line gets structured⁵⁸ and its line width follows a Curie law⁵⁹.

In the overdoped sample the behavior of the linewidth is completely different from that of the optimally doped (see Fig. 5). The pristine sample displays a completely flat $\Delta\nu(T)$ down to 9 K and then a rapid increase, likely due to the freezing of the vortex motions⁶⁰. In the irradiated sample ($\phi = 6.4 \times 10^{16} \text{ cm}^{-2}$) $\Delta\nu$ reaches a maximum around 18 K and then decreases slightly at lower temperatures. Interestingly the temperature at which the line width of the irradiated sample starts to decrease is very near to the temperature T^* at which the spin-spin relaxation rate starts to rise and the echo decay becomes a single exponential. This suggests that the low frequency spin fluctuations, which are responsible for the $1/T_2$ enhancement, partially average out the static frequency distribution probed by the ^{75}As nuclei.

We will now discuss the effect of irradiation on $1/T_2$. The marked increase of $1/T_2$ starting at $T^* > T_c$ seems to be a common feature of several 122 compounds^{37,38,60}. In Ref. 38 we showed that this effect is unrelated to the superconducting state and that T^* can become much higher than T_c in the presence of a high magnetic field. As we already explained in the previous section the $1/T_2$

enhancement below T^* is affected by proton irradiation. The increase in $1/T_2$ was associated with slow nematic fluctuations between $(\pi, 0)$ and $(0, \pi)$ ground states, very much akin to the nematic fluctuations found in prototypes of the J_1 - J_2 model on a square lattice.^{61,62} These low-frequency fluctuations have been predicted⁶³ in the iron based superconductors and nematic fluctuations have subsequently been observed in several underdoped⁶⁴⁻⁶⁶ and overdoped IBS^{37,38}.

In the presence of these fluctuations $1/T_2$ can be written as:

$$\frac{1}{T_2} = a(\Delta\nu(T))^2\tau_D(T) + \frac{1}{T_{2i}} \quad (7)$$

with τ_D the characteristic fluctuation time, a a dimensionless coupling constant and T_{2i} the T -independent contribution to the relaxation arising from nuclear dipole-dipole interaction. The resulting temperature dependent $\tau_D(T)$ can then be fitted to an Arrhenius law $\tau_D(T) = \tau_0 e^{U/T}$ where U is the activation energy and τ_0 , the high temperature characteristic time of the fluctuations, in the nanosecond range. We fitted the $1/T_2$ data using Eq. 7 in the 20 - 26 K temperature range for $x=0.068$ and in the 7 K - 30 K range for $x=0.107$.

In the pristine samples we found that, for $x=0.068$, the activation energy is $U \simeq 200 \pm 30$ K while in the overdoped $x=0.107$ sample $U \simeq 40 \pm 20$ K, in good agreement with the values obtained in Ref. 37 and 38. Upon proton irradiation U increases markedly in the optimally doped sample ($U \sim 500 \pm 100$ K for $\phi = 3.2 \times 10^{16} \text{ cm}^{-2}$) while it remains basically unchanged in the overdoped sample. Unfortunately, the quality of the fit decreases with increasing dose, pointing out that possibly the dynamics can no longer be described by a single activation barrier and that a distribution of energy barriers should be considered. This fact is particularly evident in the overdoped sample where the increase of $1/T_2$ becomes significantly sharper and T^* decrease by ~ 5 K (Fig. 6). The sub-

stantial enhancement of the activation energy suggests that the presence of the defects slows down the fluctuations between the $(0, \pi)$ and $(\pi, 0)$ ground states. It is remarked that such an effect has also been detected in the prototypes of the J_1 - J_2 model on a square lattice doped with nonmagnetic impurities.⁶⁷

IV. CONCLUSIONS

In conclusion, we have shown that proton irradiation (5.5 MeV) in $\text{Ba}(\text{Fe}_{1-x}\text{Rh}_x)_2\text{As}_2$ results in a very weak T_c suppression, in good agreement with previous experiments carried out in other 122 compounds^{13,14}. By measuring the ⁷⁵As NMR spectra we have evidenced that the defects introduced by proton irradiation induce ferromagnetic correlations in the optimally electron doped $x=0.068$ compound. Remarkably this effect is totally absent in the overdoped sample owing to the absence of significant spin correlations. Moreover the analysis of the spin echo decay rate ($1/T_2$) show that the low-frequency fluctuations observed^{33,34,64-66} in several families of iron based superconductors are damped by the irradiation induced impurities, consistently with the hypothesis that they could be associated with the presence of nematic fluctuations between $(0, \pi)$ and $(\pi, 0)$ nematic phases.

ACKNOWLEDGMENTS

This work was supported by MIUR-PRIN2012 Project No. 2012X3YFZ2 and MIUR-PRIN2015 Project No. 2015C5SEJJ. The irradiations were performed in the framework of the INFN-Politecnico di Torino M.E.S.H. Research Agreement. The work at the Ames Laboratory was supported by the DOE-Basic Energy Sciences under Contract No. DE-AC02-07CH11358. The authors wish to thank the INFN-LNL staff for their support in the irradiation experiments.

* matteo.moroni01@universitadipavia.it

- ¹ F. Masee, P. Oliver Sprau, Y.-L. Wang, J. C. S. Davis, G. Ghigo, G. Gu, W.-K. Kwok, *Science Advances* **1**, e1500033 (2015).
- ² T. Tamegai, T. Taen, H. Yagyuda, Y. Tsuchiya, S. Mohan, T. Taniguchi, Y. Nakajima, S. u Okayasu, M. Sasase, H. Kitamura, T. Murakami, T. Kambara and Y. Kanai, *Supercond. Sci. Technol.* **25**, 084008 (2012).
- ³ G. P. Summers E. A. Burke D. B. Chrisey M. Nastasi and J. R. Tesmer, *Appl. Phys. Lett.* **55**, 1469 (1989).
- ⁴ F. Rullier-Albenque, P. A. Vieillefond, H. Alloul, A. W. Tyler, P. Lejay and J. F. Marucco, *Europhys. Lett.* **50**, 81 (2000).
- ⁵ R. J. Radtke, K. Levin, H.-B. Schüttler, and M. R. Norman, *Phys. Rev. B* **48**, 653(R) (1993).
- ⁶ R. Prozorov, M. A. Tanatar, B. Roy, N. Ni, S. L. Bud'ko, P. C. Canfield, J. Hua, U. Welp, and W. K. Kwok *Phys. Rev. B* **81**, 094509 (2010)
- ⁷ N. W. Salovich, Hyunsoo Kim, Ajay K. Ghosh, R. W. Giannetta, W. Kwok, U. Welp, B. Shen, S. Zhu, H.-H. Wen, M. A. Tanatar, and R. Prozorov *Phys. Rev. B* **87**, 180502(R) (2013).
- ⁸ F. Laviano, R. Gerbaldo, G. Ghigo, L. Gozzelino, G. P. Mikitik, T. Taen and T. Tamegai, *Supercond. Sci. Technol.* **27**, 044014 (2014).
- ⁹ N. Haberkorn, Jeehoon Kim, B. Maiorov, I. Usov, G. F. Chen, W. Yu and L. Civale, *Supercond. Sci. Technol.* **27**, 095004 (2014).
- ¹⁰ F. Ohtake, T. Taen, S. Pyon, T. Tamegai, S. Okayasu, *Physics Procedia* **58**, 122-125 (2014)
- ¹¹ K. J. Kihlstrom, L. Fang, Y. Jia, B. Shen, A. E. Koshelev, U. Welp, G. W. Crabtree, W.-K. Kwok, A. Kayani, S. F. Zhu, and H.-H. Wen, *Appl. Phys. Lett.* **103**, 202601 (2013).

- ¹² T. Taen, H. Yagyuda, Y. Nakajima, T. Tamegai, S. Okayasu, H. Kitamura, T. Murakami, F. Laviano, G. Ghigo, *Physica C*, **484**, 62 (2013).
- ¹³ Y. Nakajima, T. Taen, Y. Tsuchiya, T. Tamegai, H. Kitamura, and T. Murakami, *Phys. Rev. B* **82**, 220504(R) (2010).
- ¹⁴ T. Taen, F. Ohtake, H. Akiyama, H. Inoue, Yue Sun, S. Pyon, T. Tamegai, and H. Kitamura, *Phys. Rev. B* **88**, 224514 (2013).
- ¹⁵ Y. Mizukami, M. Konczykowski, Y. Kawamoto, S. Kurata, S. Kasahara, K. Hashimoto, V. Mishra, A. Kreisel, Y. Wang, P. J. Hirschfeld, Y. Matsuda, and T. Shibauchi, *Nature Commun.* **5**, 5657 (2014).
- ¹⁶ R. Prozorov, M. Konczykowski, M. A. Tanatar, A. Thaler, S. L. Bud'ko, P. C. Canfield, V. Mishra, and P. J. Hirschfeld *Phys. Rev. X* **4**, 041032 (2014)
- ¹⁷ C. J. van der Beek, S. Demirdis, D. Colson, F. Rullier-Albenque, Y. Fasano, T. Shibauchi, Y. Matsuda, S. Kasahara, P. Gierlowski, and M. Konczykowski, *J. Physics Conference Series* **449**, 012023 (2013).
- ¹⁸ K. Cho, M. Konczykowski, J. Murphy, H. Kim, M. A. Tanatar, W. E. Straszheim, B. Shen, H. H. Wen, and R. Prozorov *Phys. Rev. B* **90**, 104514 (2014)
- ¹⁹ Kyil Cho, M. K. Teknowijoyo, M. A. Tanatar, Yong Liu, T. A. Lograsso, W. E. Straszheim, V. Mishra, S. Maiti, P. J. Hirschfeld, and R. Prozorov, *Science Advances.* **2**, e1600807 (2016)
- ²⁰ S. Teknowijoyo, K. Cho, M. A. Tanatar, J. Gonzales, A. E. Böhmer, O. Cavani, V. Mishra, P. J. Hirschfeld, S. L. Bud'ko, P. C. Canfield, and R. Prozorov *Phys. Rev. B* **94**, 064521 (2016)
- ²¹ I. I. Mazin, D. J. Singh, M. D. Johannes, and M. H. Du, *Phys. Rev. Lett.* **101**, 057003 (2008).
- ²² A. V. Chubukov, D. V. Efremov, and I. Eremin, *Phys. Rev. B* **78**, 134512 (2008).
- ²³ R. M. Fernandes, M. G. Vavilov, and A. V. Chubukov, *Phys. Rev. B* **85**, 140512(R) (2012).
- ²⁴ Yunkyu Bang and G. R. Stewart, arXiv:1701.00320v1
- ²⁵ G. Ghigo, G. A. Umbarino, L. Gozzelino et al, submitted
- ²⁶ J. Li, Y. Guo, S. Zhang, Y. Tsujimoto, X. Wang, C. I. Sathish, S. Yu, K. Yamaura, and E. Takayama-Muromachi, *Solid State Commun.* **152**, 671 (2012).
- ²⁷ Y. K. Li, X. Lin, Q. Tao, C. Wang, T. Zhou, L. Li, Q. Wang, M. He, G. Cao, and Z. A. Xu, *New J. Phys.* **11**, 053008 (2009).
- ²⁸ Y. K. Li, J. Tong, Q. Tao, C. Feng, G. Cao, W. Chen, F. C. Zhang, and Z. A. Xu, *New J. Phys.* **12**, 083008 (2010).
- ²⁹ Y. F. Guo, Y. G. Shi, S. Yu, A. A. Belik, Y. Matsushita, M. Tanaka, Y. Katsuya, K. Kobayashi, I. Nowik, I. Felner, V. P. S. Awana, K. Yamaura, and E. Takayama-Muromachi, *Phys. Rev. B* **82**, 054506 (2010).
- ³⁰ H. Kim, M. A. Tanatar, W. E. Straszheim, K. Cho, J. Murphy, N. Spyrison, J.-Ph. Reid, Bing Shen, Hai-Hu Wen, R. M. Fernandes, and R. Prozorov *Phys. Rev. B* **90**, 014517 (2014)
- ³¹ J.-Ph. Reid, M. A. Tanatar, X. G. Luo, H. Shakeripour, S. R. de Cotret, A. Juneau-Fecteau, J. Chang, B. Shen, H.-H. Wen, H. Kim, R. Prozorov, N. Doiron-Leyraud, and Louis Taillefer *Phys. Rev. B* **93**, 214519 (2016)
- ³² A. V. Chubukov, M. Khodas, and R. M. Fernandes, *Phys. Rev. X* **6**, 041045 (2016).
- ³³ N. J. Curro, A. P. Dioguardi, N. ApRoberts-Warren, A. C. Shockley, and P. Klavins, *New J. Phys.* **11**, 075004 (2009).
- ³⁴ H. Xiao, T. Hu, A. P. Dioguardi, N. apRoberts-Warren, A. C. Shockley, J. Crocker, D. M. Nisson, Z. Viskadourakis, X. Tee, I. Radulov, C. C. Almasan, N. J. Curro, and C. Panagopoulos, *Phys. Rev. B* **85**, 024530 (2012).
- ³⁵ A. P. Dioguardi, M. M. Lawson, B. T. Bush, J. Crocker, K. R. Shirer, D. M. Nisson, T. Kissikov, S. Ran, S. L. Bud'ko, P. C. Canfield, S. Yuan, P. L. Kuhns, A. P. Reyes, H.-J. Grafe, and N. J. Curro *Phys. Rev. B* **92**, 165116 (2015)
- ³⁶ T. Kissikov, A. P. Dioguardi, E. I. Timmons, M. A. Tanatar, R. Prozorov, S. L. Bud'ko, P. C. Canfield, R. M. Fernandes, and N. J. Curro *Phys. Rev. B* **94**, 165123 (2016)
- ³⁷ L. Bossoni, P. Carretta, W. P. Halperin, S. Oh, A. Reyes, P. Kuhns, and P. C. Canfield *Phys. Rev. B* **88**, 100503(R) (2013).
- ³⁸ L. Bossoni, M. Moroni, M. H. Julien, H. Mayaffre, P. C. Canfield, A. Reyes, W. P. Halperin, and P. Carretta, *Phys. Rev. B* **93**, 224517 (2016).
- ³⁹ N. Ni, M. E. Tillman, J.-Q. Yan, A. Kracher, S. T. Hannahs, S. L. Bud'ko, and P. C. Canfield, *Phys. Rev. B* **78**, 214515 (2008); N. Ni, A. Thaler, A. Kracher, J.-Q. Yan, S. L. Bud'ko, and P. C. Canfield, *ibid.* **80**, 024511 (2009).
- ⁴⁰ M. A. Tanatar, N. Ni, C. Martin, R. T. Gordon, H. Kim, V. G. Kogan, G. D. Samolyuk, S. L. Bud'ko, P. C. Canfield, and R. Prozorov, *Phys. Rev. B* **79**, 094507 (2009).
- ⁴¹ M. A. Tanatar, N. Ni, S. L. Bud'ko, P. C. Canfield, and R. Prozorov, *Supercond. Sci. Technol.* **23**, 054002 (2010).
- ⁴² M. A. Tanatar, R. Prozorov, N. Ni, S. L. Bud'ko, P. C. Canfield, U.S. Patent 8,450,246.
- ⁴³ M. A. Tanatar, N. Ni, A. Thaler, S. L. Bud'ko, P. C. Canfield, and R. Prozorov, *Phys. Rev. B* **82**, 134528 (2010).
- ⁴⁴ J.F. Ziegler, <http://www.srim.org/>.
- ⁴⁵ A. G. Redfield and W. N. Yu, *Phys. Rev.* **169**, 443 (1968).
- ⁴⁶ R. E. Walstedt and S.-W. Cheong, *Phys. Rev. B* **51**, 3163 (1995).
- ⁴⁷ S. Mukhopadhyay, S. Oh, A. M. Mounce, M. Lee, W. P. Halperin, N. Ni, S. L. Bud'ko, P. C. Canfield, A. P. Reyes and P. L. Kuhns, *New Journal of Physics* **11**, 055002 (2009).
- ⁴⁸ A. Abragam, *Principles of Nuclear Magnetism* (Oxford University Press), New York (1961).
- ⁴⁹ H. Alloul, J. Bobroff, M. Gabay, and P. J. Hirschfeld, *Rev. Mod. Phys.* **81**, 45 (2009).
- ⁵⁰ D. LeBoeuf, Y. Texier, M. Boselli, A. Forget, D. Colson, and J. Bobroff, *Phys. Rev. B* **89**, 035114 (2014).
- ⁵¹ Y. Texier, Y. Laplace, P. Mendels, J. T. Park, G. Friemel, D. L. Sun, D. S. Inosov, C. T. Lin and J. Bobroff, *EPL*, **99**, 17002 (2012).
- ⁵² P. Wiecki, B. Roy, D. C. Johnston, S. L. Bud'ko, P. C. Canfield, and Y. Furukawa *Phys. Rev. Lett.* **115**, 137001 (2015).
- ⁵³ J. Cui, P. Wiecki, S. Ran, S. L. Bud'ko, P. C. Canfield, and Y. Furukawa *Phys. Rev. B* **94**, 174512 (2016).
- ⁵⁴ F. Hammerath, M. Moroni, L. Bossoni, S. Sanna, R. Kappenberger, S. Wurmehl, A. U. B. Wolter, M. A. Afrassa, Y. Kobayashi, M. Sato, B. Büchner, and P. Carretta, *Phys. Rev. B* **92**, 020505(R) (2015).
- ⁵⁵ M. Moroni, S. Sanna, G. Lamura, T. Shiroka, R. De Renzi, R. Kappenberger, M. A. Afrassa, S. Wurmehl, A. U. B. Wolter, B. Büchner, and P. Carretta, *Phys. Rev. B* **94**, 054508 (2016).
- ⁵⁶ P. Esquinazi, W. Hergert, D. Spemann, A. Setzer, and A. Ernst, *Transaction on Magnetics* **49** (8), 4668 (2013).

- ⁵⁷ T. Goko, A. A. Aczel, E. Baggio-Saitovitch, S. L. Bud'ko, P. C. Canfield, J. P. Carlo, G. F. Chen, Pengcheng Dai, A. C. Hamann, W. Z. Hu, H. Kageyama, G. M. Luke, J. L. Luo, B. Nachumi, N. Ni, D. Reznik, D. R. Sanchez-Candela, A. T. Savici, K. J. Sikes, N. L. Wang, C. R. Wiebe, T. J. Williams, T. Yamamoto, W. Yu, and Y. J. Uemura, *Phys. Rev. B* **80**, 024508 (2009).
- ⁵⁸ H. Alloul, P. Mendels, H. Casalta, J. F. Marucco, and J. Arabski, *Phys. Rev. Lett.* **67**, 3140 (1991).
- ⁵⁹ A. V. Mahajan, H. Alloul, G. Collin, and J. F. Marucco, *Phys. Rev. Lett.* **72**, 3100 (1994).
- ⁶⁰ S. Oh, A. M. Mounce, S. Mukhopadhyay, W. P. Halperin, A. B. Vorontsov, S. L. Bud'ko, P. C. Canfield, Y. Furukawa, A. P. Reyes, and P. L. Kuhns, *Phys. Rev. B* **83**, 214501 (2011).
- ⁶¹ P. Carretta, R. Melzi, N. Papinutto, and P. Millet, *Phys. Rev. Lett.* **88**, 047601 (2002).
- ⁶² P. Chandra, P. Coleman, and A. I. Larkin *Phys. Rev. Lett.* **64**, 88 (1990).
- ⁶³ I. I. Mazin and M. D. Johannes, *Nat. Phys.* **5**, 141 (2009).
- ⁶⁴ M. Fu, D. A. Torchetti, T. Imai, F. L. Ning, J.-Q. Yan, and A. S. Sefat, *Phys. Rev. Lett.* **109**, 247001 (2012).
- ⁶⁵ T. Iye, M.-H. Julien, H. Mayaffre, M. Horvatić, C. Berthier, K. Ishida, H. Ikeda, S. Kasahara, T. Shibauchi, and Y. Matsuda, *J. Phys. Soc. Jpn.* **84**, 043705 (2015).
- ⁶⁶ R. Zhou, L. Y. Xing, X. C. Wang, C. Q. Jin, and Guo-qing Zheng, *Phys. Rev. B* **93**, 060502 (2016).
- ⁶⁷ N. Papinutto, P. Carretta, S. Gonthier, and P. Millet, *Phys. Rev. B* **71**, 174425 (2005).